FOLIA HISTOCHEMICA ET CYTOBIOLOGICA
Vol. 59, No. 4, 2021
pp. 259–270

ORIGINAL PAPER

VIA MEDICA

Tanshinone IIA attenuates high glucose-induced epithelial-to-mesenchymal transition in HK-2 cells through VDR/Wnt/β-catenin signaling pathway

Jingyi Zeng, Xiaorong Bao

[1]Department of Nephrology, Jinshan Hospital, Fudan University, Shanghai, China

Abstract

Introduction. The progression of diabetic kidney disease (DKD) is closely related to renal tubular epithelial-to-mesenchymal transition (EMT) and tubulointerstitial fibrosis. Tanshinone IIA (TSIIA), extracted from a traditional Chinese medicine named Salvia miltiorrhiza, has been proved to have anti-fibrosis effects. The aim of this study was to investigate the effect of TSIIA on high glucose-induced EMT in human proximal tubular cells (HK-2 cells) and its possible mechanism.

Material and methods. The proliferation of cells exposed to different concentrations of glucose was measured by light microscopy and CCK-8 test. The cells were stimulated with 30 mM glucose and different concentrations of TSIIA (5 μM or 10 μM) for 48 h. Vitamin D receptor (VDR)-siRNA was used to transfect cells, and high glucose and TSIIA treatment were further used to treat cells. The expression of alpha smooth muscle actin (α-SMA) mRNA was detected by qPCR to ensure successful induction of EMT, and the expression of VDR mRNA was detected by qPCR to ensure successful transfection of VDR-siRNA. Protein expression of α-SMA, E-cadherin, VDR, β-catenin and glycogen synthase kinase 3β (GSK-3β) was detected by Western blot analysis.

Results. The results showed that high glucose concentration inhibited cell proliferation and promoted EMT in HK-2 cells. TSIIA could reverse high glucose-induced EMT by increasing the level of VDR protein and inhibiting the levels of β-catenin and GSK-3β proteins suggestive of a negative correlation between VDR and the Wnt/β-catenin pathway. After VDR-siRNA transfection and incubation of cells at high glucose concentration, the inhibitory effect of VDR on the expression of β-catenin and GSK-3β of Wnt pathway was suppressed and the β-catenin pathway was activated. When VDR level was restored by TSIIA, the inhibitory effect of VDR on the pathway was also restored and the activation of the pathway was suppressed.

Conclusions. TSIIA was able to attenuate high glucose-induced EMT in HK-2 cells by up-regulating VDR levels, which might be related to the inhibitory effect of VDR on the Wnt pathway. *(Folia Histochemica et Cytobiologica 2021, Vol. 59, No. 4, 259–270)*

Key words: tanshinone IIA; HK-2 cells; epithelial-to-mesenchymal transition; VDR; Wnt/β-catenin pathway

Introduction

Diabetic kidney disease (DKD), one of the most severe microangiopathy in diabetes, has become the first leading cause of end-stage renal disease (ESRD) with its increasing incidence rate all over the world. Thus, it is urgent to explore the specific mechanism and find out the specific targets of DKD.

DKD is characterized by glomerulosclerosis and tubulointerstitial fibrosis at its end-stage. In recent years, epithelial-to-mesenchymal transition (EMT) is considered to be closely related to tubulointerstitial fibrosis, which is characterized by the loss of E-cadherin expression and the increased expression of alpha smooth muscle actin (α-SMA), vimentin and fibronectin [1]. The normal expression of E-cadherin is

Correspondence address: Xiao-Rong Bao,
Department of Nephrology, Jinshan Hospital,
Fudan University,
No. 1508, Longhang Road, Jinshan District, 200540 Shanghai, China
e-mail: xrbao19660108@163.com

Folia Histochem Cytobiol. 2021
10.5603/FHC.a2021.0025
ISSN 0239-8508, e-ISSN 1897-5631

www.journals.viamedica.pl/folia_histochemica_cytobiologica

significant for epithelial cells to perform their normal functions, and α-SMA can be abundantly expressed in mesenchymal cells. EMT plays an important role in the progression of DKD to ESRD [2]. Therefore, suppressing EMT is of great importance for inhibiting tubulointerstitial fibrosis and preventing the occurrence and development of DKD.

Previous studies have suggested that the activation of the Wnt/β-catenin signaling pathway is highly involved in the process of various organ fibrosis [3] such as renal [4], liver [5], peritoneal [6], and dermal fibrosis [7]. Studies also found that the upregulation of the vitamin D receptor (VDR) might contribute to the alleviation of organ fibrosis [8]. Moreover, VDR gene can regulate the expression of many genes, and the analysis of Targetscan database by Cong [9] suggested that Wnt gene and β-catenin gene may be potential targets of VDR protein. This theoretical analysis makes the basis for the elucidation of the relationship between VDR and the Wnt signaling pathway in EMT of DKD.

Due to few available treatments and limited efficacy of drugs for DKD, there is a strong need to explore safe and effective drugs for clinical application. Traditional Chinese medicine is a treasure-house in China because of its therapeutic potential and relative safety. Tanshinone IIA (TSIIA) [10], derived from the dried root and rhizome of Salvia miltiorrhiza Bge., is one of the major active ingredients of Salvia miltiorrhiza [11]. TSIIA has been reported to protect against a variety of diseases through its various pharmacological actions, especially, anti-fibrotic, antiproliferative and anti-inflammatory effects [12]. Feng *et al.* [13] identified that TSIIA alleviated cardiac hypertrophy in spontaneously hypertensive rats by inhibiting the Wnt signaling pathway. Li *et al.* [14] clarified that TSIIA could be used to treat pituitary adenoma by downregulating the Wnt signaling pathway in AtT-20 cells. It has been found that TSIIA can inhibit the Wnt pathway. However, what is the efficacy of tanshinone IIA in DKD and whether its activity is related to VDR and the Wnt pathway remains to be further studied. Therefore, our study aimed to explore the efficacy of TSIIA on high glucose-induced EMT in HK-2 cells, a cell line obtained from the Cell Bank of the Chinese Academy of Sciences (Shanghai, China), and to investigate the regulation mechanism of it on VDR and the Wnt pathway.

Materials and methods

Reagents. D-(+)-Glucose (G8270-100G), dimethyl sulfoxide (DMSO, D2650-5X5ML), TSIIA (T4952-5MG, ≥ 97%(HPLC)) and fetal bovine serum (FBS, F8687-500ML) were purchased from Sigma-Aldrich (St. Louis, MO, USA). RNA-Quick Purification Kit (ES-RN001), HRP-AffiniPure Goat Anti-Mouse IgG(H+L), (#SGAMHRP) and HRP-AffiniPure Goat Anti-Rabbit IgG(H+L(#SGARHRP) was purchased form Yishan Biotechnology (Shanghai, China). PrimeScript™ RT Master Mix (Perfect Real Time, RR036A) and TB Green™ Premix Ex Taq™ (Tli RNaseH Plus, RR820A) were purchased from TAKARA (Tokyo, Japan). SDS lysis buffer (P0013G) was purchased from Beyotime Biotechnology (Shanghai, China). Low-glucose (5.56mM) Dulbecco's modified Eagle medium (DMEM, KGM31600-500), PMSF (KGP610), PI (KGP602), BCA Protein Assay Kit (KGP902) and the Cell Counting Kit-8 (CCK-8, KGA317) were purchased from KeyGEN Biotechnology (Jiangsu, China). α-SMA Rabbit mAb (#19245), GSK-3β Rabbit mAb (#12456), β-catenin Rabbit mAb (#8480), E-cadherin Mouse mAb (#14472) and VDR Rabbit mAb (#12550) were purchased from Cell Signaling Technology (CST, MA, USA), E-cadherin Mouse mAb (#ab231303) was purchased from Abcam (MA, USA). Primers were purchased from Sangon Biotech (Shanghai, China). VDR small interfering (siRNA) and riboFECT™ CP Transfection Kit (#C10511-1) were purchased from RiboBio (Guangzhou, China). GAPDH Mouse mAb (#M20006F) was presented by Abmart (Shanghai, China).

Cell culture. The immortalized human proximal tubular cells (HK-2 cells, SCSP-511), obtained from the Cell Bank of the Chinese Academy of Sciences (Shanghai, China) on 25 August 2020, were cultured in low-glucose 5.56 mM DMEM medium supplemented with 10% FBS. The culture condition of the incubator was maintained at 37°C with 5% CO_2. The medium was changed every 2 days, and the cells were passaged 4-5 the confluence of them was about 80–90% (every 4–5 days). The cells within ten generations were used for the experiments.

Cell proliferation assay. The number of HK-2 cells in the cell suspensions was counted by cell counting chamber, and then these cells (3×10^3/100 μl/well) were seeded into a 96-well plate and cultured in DMEM medium with 10% FBS for 24 h. The next 8 hours, the cells were cultured in serum-free DMEM medium. After that, HK-2 cells were cultured in DMEM medium at different concentrations of glucose (5.56 mM, 20 mM, 30 mM, 40 mM, 50 mM) for 48 h. Each experimental group was set with 6 duplicate wells. According to the manufacturer's instructions, 10 μl CCK-8 solution was added into each well, and the cell viability was measured by reading the OD value at 450 nm after 1 h of incubation. After removing the highest value and lowest value in each group, the remaining four values were taken for calculation.

Cell treatment and transfection. HK-2 cells were evenly seeded into 6-well plates at the density of 5×10^4 cells

Folia Histochem Cytobiol. 2021
10.5603/FHC.a2021.0025
ISSN 0239-8508, e-ISSN 1897-5631

Table 1. The sequences of VDR-siRNA

Product number	Product name	Target sequences (5'-3')
siG101230160723	VDR-siRNA003	GCTCGAAGTGTTTGGCAAT
stB0005376A	VDR-siRNA001	AGCGCATCATTGCCATACT
stB0005376B	VDR-siRNA002	GTCAGTTACAGCATCCAAA

Table 2. The preparation of transfection complexes

Group	SiRNA	RiboFECT™CP Buffer(1X)	RiboFECT™CP Reagent		DMEM medium
Blank	None	None	None	Mixed and incubated for 15 min at room temperature	1 ml
NC	2.5 μl NC siRNA	60 μl	6 μl		931.5 μl
siVDR1	2.5 μl VDR-siRNA001	60 μl	6 μl		931.5 μl
siVDR2	2.5 μl VDR-siRNA002	60 μl	6 μl		931.5 μl
siVDR3	2.5 μl VDR-siRNA003	60 μl	6 μl		931.5 μl

per well for 24 h. After HK-2 cells were incubated with serum-free medium for 8 h, they were randomly divided into the following four groups and cultured for 48 h: control group (5.56 mM glucose in the medium), high glucose (HG) group (30 mM glucose in the medium), HG TSIIA-5 group (30 mM glucose + 5 μM TSIIA in the medium), and HG TSIIA-10 group (30 mM glucose + 10 μM TSIIA in the medium).

According to the protocols of the transfection kit, the siRNA powder was configured into 20 μM storage solution. The target sequences of VDR-siRNA were exhibited in Table 1. HK-2 cells (5×10^4/well) were plated in 6-well plates and incubated for 24 h. Then they were transfected with 50 nM transfection complexes when the cell density ranged from 30% to 50%. The preparation of 50 nM transfection complexes was shown in Table 2. Firstly, 2.5 μL solution of different siRNA (NC, VDR-siRNA001, VDR-siRNA002, VDR-siRNA003) was diluted with 60 μL ribo*FECT*™CP Buffer(1X). Then this solution was mixed gently and incubated for 15 min at room temperature after adding 6 μL ribo*FECT*™CP Reagent. Finally, to prepare 50 nM transfection complexes, 931.5 μL serum-free DMEM medium was added into above mixture. After 6 h of transfection and 8 h of serum-free medium treatment, HK-2 cells were cultured in DMEM medium (containing 5.56 mM glucose) for 48 h. According to the expression of VDR mRNA in transfected HK-2 cells, the most effective sequence to silence VDR gene was selected for the subsequent experiments.

By the method described above, HK-2 cells were transfected after one day of incubation. Then they were randomly divided into the following five groups and cultured for 48 h with or without 30 mM glucose and 5 μM TSIIA: blank group (no treatment), negative control group (NC group, NC-siRNA transfection), siVDR group (VDR-siRNA003 transfection), siVDR + HG group (VDR-siRNA003 transfection + 30 mM glucose) and siVDR + HG + T5 group (VDR-siRNA003 transfection + 30 mM glucose + 5 μM TSIIA).

Microscopic examination. HK-2 cells were treated as described above, and the morphological changes of cells induced by different treatments were observed under the Olympus IX73 microscope (Olympus, Tokyo, Japan), such as the size, shape and density of cells.

Quantitative real-time polymerase chain reaction (qRT-PCR). The total RNA was extracted from HK-2 cells using the RNA-Quick Purification Kit. The concentration and purity of extracted RNA were detected to ensure that the concentration was not less than 30 ng/μl and A260/A280 was between 1.90 and 2.20. Then the cDNA was obtained by reverse transcription using TAKARA RR036A. Next, qRT-PCR was carried out in strict accordance with the instructions of TAKARA RR820A and the Applied Biosystems 7300 Fast Real-Time PCR System. $2^{-\Delta\Delta Ct}$ method was subsequently performed to calculate the relative expression of target genes. The sequences of primers were exhibited in Table 3.

Western blotting. The total protein was extracted from HK-2 cells using SDS lysis buffer containing phenylmethyl sulfonylfluoride (PMSF) and phosphatase inhibitors (PI). The supernatant was obtained after the cells was treated three times (2 sec each time) with ultrasonic fragmentation (ice bath for 10 s after each operation) and centrifuged at 15000 g for 10 min. Before the protein was added with SDS-PAGE Sample loading buffer and boiled for denaturation, the concentration of the cells total protein was measured by BCA Protein Assay Kit (KGP902, KeyGEN Biotechnology, Jiangsu, China). Then 20 μg of proteins were loaded on 10%

Table 3. The sequences of primers for quantitative real-time PCR analysis

Gene	Forward Primer (5'-3')	Reverse Primer (5'-3')
β-actin	AGGCACCAGGGCGTGAT	GCCCACATAGGAATCCTTCTGAC
α-SMA	GGGAATGGGACAAAAAGACA	CTTCAGGGGCAACACGAA
VDR	GGTGGAGGGAGCCATCCTT	TGGGACAGCTCTAGGGTCACA

α-SMA — alpha smooth muscle actin; VDR — vitamin D receptor

SDS-PAGE and transferred to PVDF membranes. Next, the membranes were blocked in QuickBlock™ blocking buffer at room temperature for 15 min and incubated with the following primary antibodies (1:1000) at 4°C overnight: α-SMA Rabbit mAb (#19245, Cell Signaling Technology, MA, USA), GSK-3β Rabbit mAb (#12456, Cell Signaling Technology, MA, USA), β-catenin Rabbit mAb (#8480, Cell Signaling Technology, MA, USA), E-cadherin Mouse mAb (#ab231303,Abcam, MA, USA), VDR Rabbit mAb (#12550, Cell Signaling Technology, MA, USA) and GAPDH Mouse mAb (#M20006F, Abmart, Shanghai, China). After washing with TBST three times, the membranes were incubated with corresponding secondary antibodies (HRP-AffiniPure Goat Anti-Mouse IgG(H+L) (#SGAMHRP, Yishan, Shanghai, China), HRP-AffiniPure Goat Anti-Rabbit IgG(H+L) (#SGARHRP, Yishan, Shanghai, China) (1:5000) at room temperature for 1 h. The expression level of proteins was detected by Chemiluminescent detection and analyzed by Image-J (NIH, Bethesda, MD, USA).

Statistical analysis. All experiments were repeated three times independently (n = 3). Statistical analysis was performed using GraphPad Prism 8.0.2 (GraphPad Software, San Diego, CA, USA). All data were presented as the mean ± standard deviation (SD). Shapiro-Wilk test was used to test whether the statistics meet the normal distribution, and then ordinary one-way ANOVA with Tukey test was utilized to estimate statistically significant differences. $P < 0.05$ was considered to be statistically significant.

Results

Determination of suitable glucose concentration for the induction of EMT

To determine the best glucose concentration to induce EMT in HK-2 cells, the cells were exposed to different concentrations of glucose (5.56 mM, 20 mM, 30 mM, 40 mM, 50 mM) for 48 h. Then the protein expressions of E-cadherin and β-catenin in HK-2 cells were identified by Western blot and the cell proliferation was measured by CCK-8 test. We found that the protein expression of E-cadherin significantly decreased, and the protein expression of β-catenin significantly increased when cells were exposed to glucose at concentrations of 30 mM and 40 mM (Fig. 1A). Also, the cell proliferation was significantly inhibited at these different concentrations of glucose (Fig. 1B). Because 30 mM glucose inhibited E-cadherin protein expression in HK-2 cells, and the viability of cells cultured with 30 mM glucose was higher than that with 40 mM glucose, we chose 30 mM as the most suitable concentration of the model condition and designed it as 'high glucose' (HG).

High glucose induces EMT in HK-2 cells

The expressions of α-SMA and E-cadherin are considered to be closely associated with the progression of EMT. Thus, to confirm whether EMT model was successfully established, we first detected the total protein expressions of α-SMA and E-cadherin by Western blot analyses. The Western blot results suggested that the protein level of α-SMA in HG group was significantly increased compared with that in the control group (Fig. 2A–B). In addition, compared with the control group, the E-cadherin protein level in the HG group decreased (Fig. 2C–D). These results indicated that 30 mM glucose successfully induced EMT in HK-2 cells, and an *in vitro* EMT model was successfully established.

Tanshinone IIA attenuates EMT induced by high glucose in HK-2 cells

To evaluate the role of TSIIA in HG-induced EMT cells, the cells were incubated with 30 mM glucose and different concentrations of TSIIA (5 μM or 10 μM) for 48 h. We observed their morphological changes by light microscopy and measured the expressions of EMT-related markers by qPCR and Western blot. As shown in Figure 1A, we found that the abnormal morphology of cells at high glucose concentration disappeared after their incubation with TSIIA. Also, the cell density in both TSIIA-5 group and TSIIA-10 group reverted and increased. Furthermore, the morphological changes of cells were further improved when TSIIA concentration was increased from 5 μM to 10 μM. As shown in Figure 2A, the increased α-SMA protein expressions in HG group were markedly reversed by TSIIA. In addition, α-SMA protein expressions in the TSIIA-10 group were lower than those in the TSIIA-5 group.

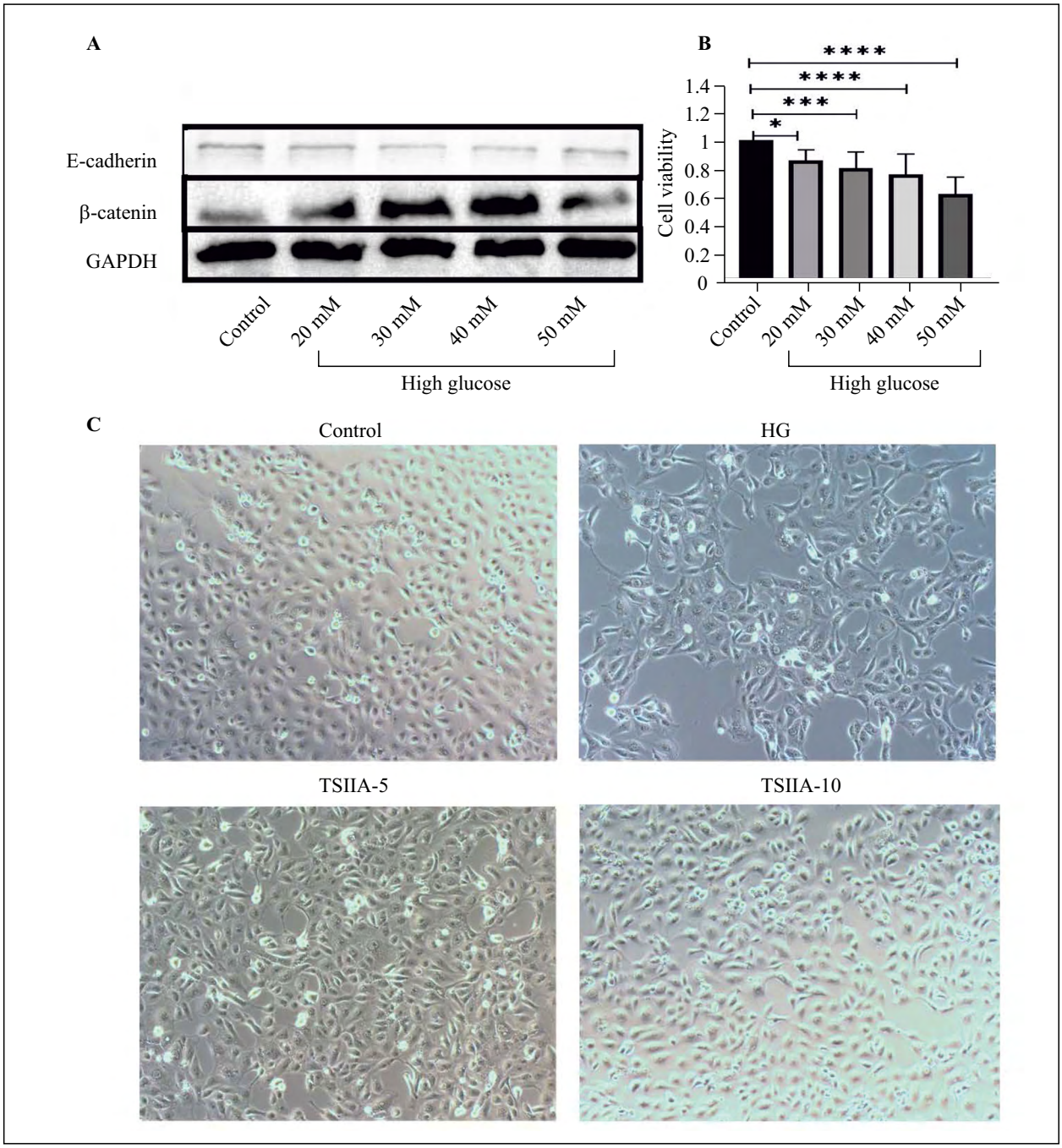

Figure 1. Effects of high glucose (HG) and tanshinone IIA (TSIIA) on HK-2 cells. **A.** The protein expression of E-cadherin and β-catenin in HK-2 cells exposed to different concentrations of glucose (5.56 mM, 20 mM, 30 mM, 40 Mm, 50 mM). **B.** The viability of HK-2 cells exposed to the indicated concentrations of glucose (5.56 mM, 20 mM, 30 mM, 40 Mm, 50 mM). **C.** The morphological changes of cells exposed to glucose and TSIIA. All data are presented as mean ± SD (n = 3). $^{*}P < 0.05$, $^{**}P < 0.01$, $^{***}P < 0.001$.

Besides, in striking contrast to HG treatment, TSIIA treatment significantly increased the E-cadherin protein levels (Fig. 2A–B), proportionally to the TSIIA concentration. To sum up, it showed that TSIIA could attenuate HG-induced EMT features in HK-2 cells, and its effect was concentration-dependent.

Tanshinone IIA inhibits EMT by upregulating VDR and suppressing Wnt signaling pathway

To further explore the mechanism of EMT, we examined the protein expressions of VDR, β-catenin and GSK-3β *via* Western blots. According to Figures 2A, 2C–E, the VDR protein content in

Folia Histochem Cytobiol. 2021
10.5603/FHC.a2021.0025
ISSN 0239-8508, e-ISSN 1897-5631

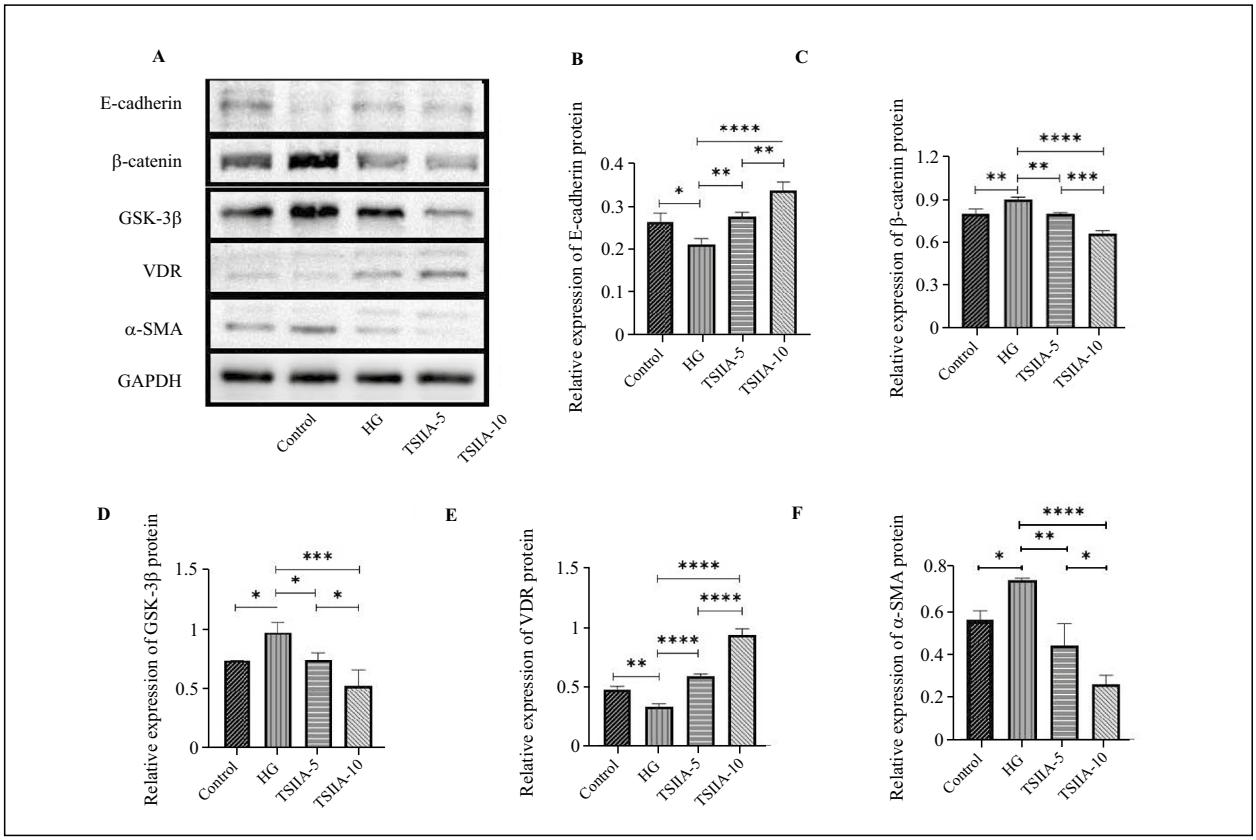

Figure 2. The protein levels of HK-2 cells were detected by Western blot. **A.** The protein levels of alpha smooth muscle actin (α-SMA), E-cadherin, vitamin D receptor (VDR), β-catenin and glycogen synthase kinase 3β (GSK-3β). **B.** The relative expression of E-cadherin protein. **C.** The relative expression of β-catenin protein. **D.** The relative expression of GSK-3β protein. **E.** The relative expression of VDR protein. **F.** The relative expression of α-SMA protein. All data are presented as mean ± SD (n = 3). $^{*}P < 0.05$, $^{**}P < 0.01$, $^{***}P < 0.001$, $^{****}P < 0.0001$.

the HG group was significantly lower than that in the control group, while the β-catenin and GSK-3β protein contents in the HG group were significantly higher than those in the control group. These findings showed that VDR and Wnt/β-catenin pathways might participant in the development of EMT in HK-2 cells and we decided to explore the role of TSIIA in this process. Compared with the induction of EMT by HG, the TSIIA treatment clearly upregulated the VDR protein levels and downregulated the β-catenin and GSK-3β protein levels (Fig. 2A, 2C–E). Moreover, these processes were more obvious in TSIIA-10 group than those in TSIIA-5 group. These findings strongly supported that VDR and Wnt/β-catenin pathways were involved in EMT. Moreover, there was a regulatory relationship between VDR and Wnt/β-catenin pathways. Thus, in HK-2 cells HG promoted EMT by inhibiting VDR protein levels and activating Wnt/β-catenin pathway with TSIIA producing opposite effects.

The effect of VDR-siRNA transfection on EMT in HK-2 cells

To further study the mechanisms of the relationship between VDR and Wnt/β-catenin pathways in the pathogenesis of DKD, we firstly screened out the most effective sequence to silence VDR gene from three different transfection sequences according to the expression of VDR mRNA in transfected HK-2 cells. As shown in Figure 3A, the relative expression of VDR mRNA in the blank group, NC group, siVDR-001 group, siVDR-002 group and siVDR-003 group was 0.9292 ± 0.06221, 0.9369 ± 0.1093, 0.4965 ± 0.1877, 0.5615 ± 0.08345, and 0.3682 ± 0.1036, respectively. The expression of VDR mRNA in siVDR-001 group, siVDR-002 group and siVDR-003 group was significantly lower than that in the blank group and NC group, and the VDR mRNA expression in siVDR-003 group was the lowest among them. There was no significant difference in the expression of VDR mRNA between the blank group and NC group. Therefore, siVDR-003 was selected for the subsequent experiments.

Folia Histochem Cytobiol. 2021
10.5603/FHC.a2021.0025
ISSN 0239-8508, e-ISSN 1897-5631

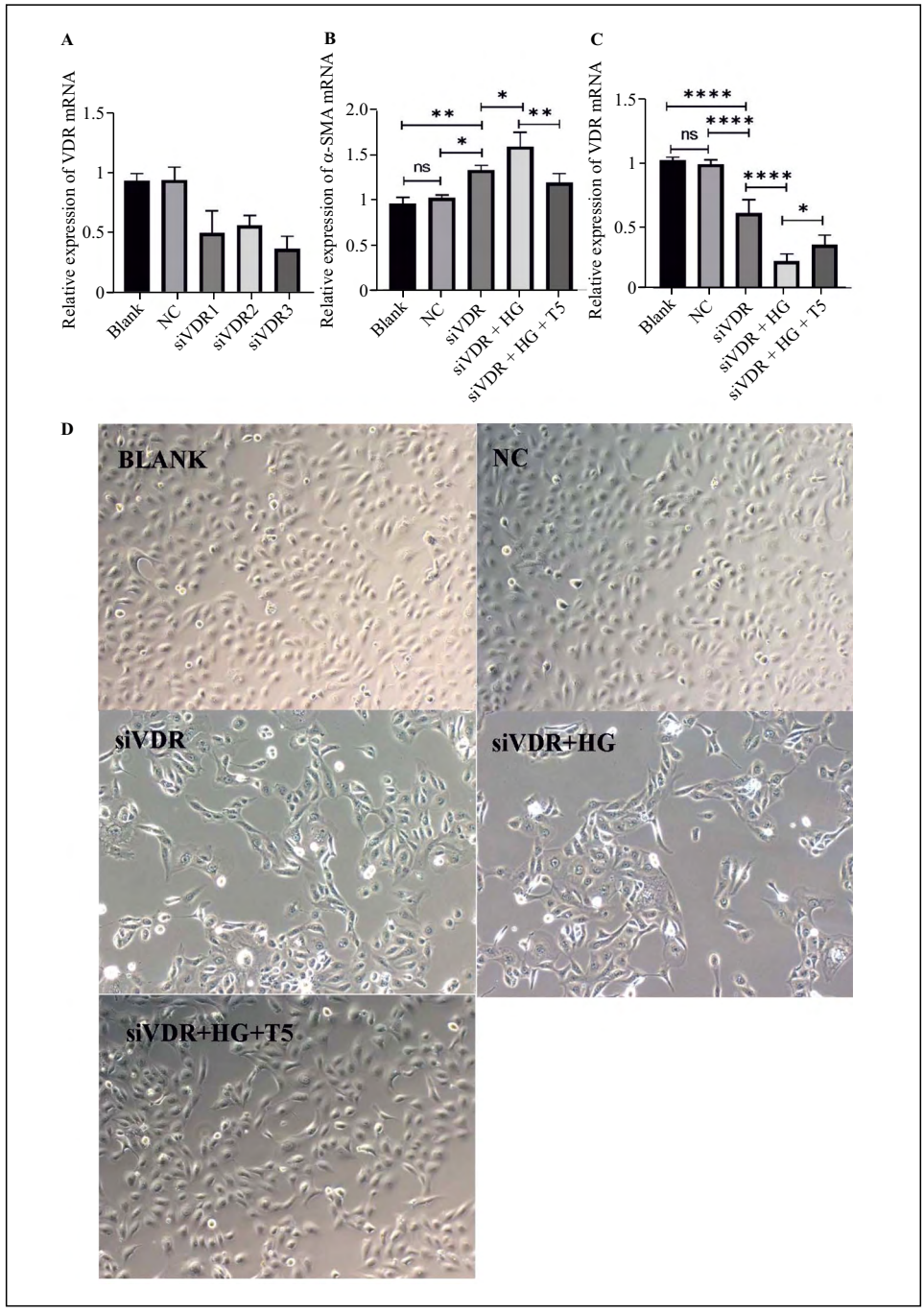

Figure 3. Tanshinone IIA ameliorated siVDR and high glucose-induced EMT on HK-2 cells. **A.** Screening out the most effective sequence to silence VDR level. **B.** The relative expression of α-SMA mRNA. **C.** The relative expression of VDR mRNA. **D.** The morphological changes of cells treated with different treatments. All data are presented as mean ± SD (n = 3). $^{*}P < 0.05$, $^{**}P < 0.01$, $^{***}P < 0.001$, $^{****}P < 0.0001$. Blank, no treatment; NC — negative control; siVDR — VDR-siRNA transfection; T5 — tanshinone IIA (5 μM).

After silencing VDR gene, the morphological changes of HK-2 cells were observed under light microscope, and the expression of EMT-related molecules in cells was determined by qPCR and Western blotting. The silencing of the VDR mRNA level in HK-2 cells resulted in the alterations of cell morphology since they became spindle-shaped, which was the same as that of mesenchymal cells (Fig. 3D). Compared to the blank group and NC group, the VDR-siRNA transfection significantly reduced the mRNA and protein levels of VDR and elevated the mRNA and protein levels of α-SMA (Fig. 3B–C, 4D–E). These results caused by VDR-siRNA transfection were highly consistent with those in-

Folia Histochem Cytobiol. 2021
10.5603/FHC.a2021.0025
ISSN 0239-8508, e-ISSN 1897-5631

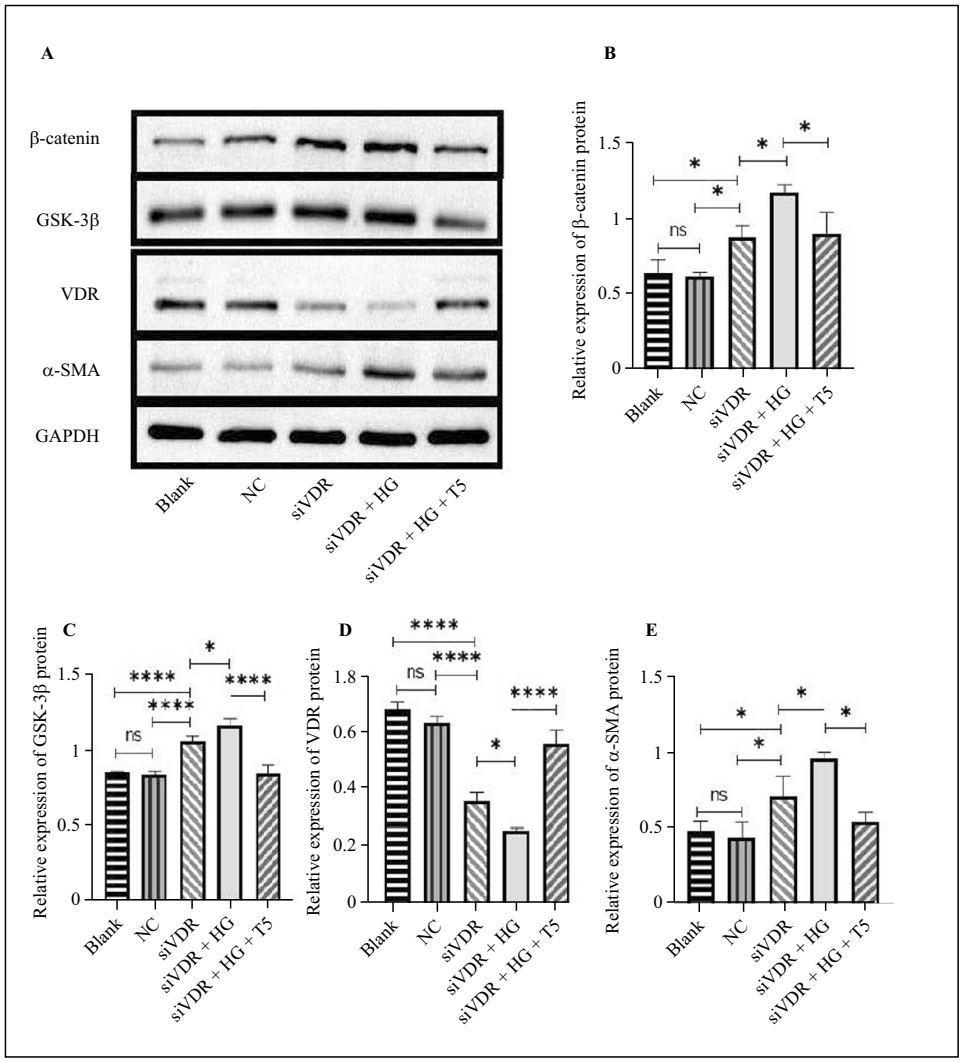

Figure 4. The protein levels of HK2 cells were analyzed by Western blot. **A.** The protein levels of α-SMA, VDR, β-catenin and GSK-3β. **B.** The relative expression of β-catenin protein. **C.** The relative expression of GSK-3β protein. **D.** The relative expression of VDR protein. **E.** The relative expression of α-SMA protein. All data are presented as mean ± SD (n = 3). $^{*}P < 0.05$, $^{**}P < 0.01$, $^{***}P < 0.001$, $^{****}P < 0.0001$.

duced by high glucose level. In addition, the protein expressions of β-catenin and GSK-3β in the siVDR group were higher than those in the blank group and NC group (Fig. 4B–C), suggesting the activation of Wnt/β-catenin pathway in siVDR-transfected cells. Collectively, silencing VDR activated Wnt/β-catenin pathway, resulting in EMT in HK-2 cells. Therefore, we hypothesized that VDR might inhibit Wnt/β-catenin pathway since with the downregulation of VDR, the inhibition by VDR of the pathway was suppressed and the Wnt/β-catenin pathway was activated.

Tanshinone IIA ameliorates siVDR- and high glucose-induced EMT through VDR/Wnt/β-catenin signaling pathway

Compared with the siVDR group, the EMT features in HK-2 cells were further aggravated in the siVDR+HG group manifesting mainly as obvious inhibition of cell proliferation (Fig. 3D). Besides, the mRNA and protein levels of α-SMA in the siVDR + HG group were remarkably higher than those in the siVDR group (Fig. 3B, 4A, 4E). These results could be reversed to a certain extent by TSIIA treatment since most of the cells returned to the morphology of control cells, and the mRNA and protein levels of α-SMA decreased significantly (Fig. 3C, 4A, 4E). Moreover, compared with the siVDR group, the expression of VDR mRNA and protein in the siVDR + HG group was obviously reduced, while the expression of β-catenin and GSK-3β protein was increased (Fig. 3C, 4B–D). Contrary to the siVDR + HG group, the expression of VDR mRNA and protein in the siVDR + HG + T5 group was significantly increased, while the expression of β-catenin and GSK-

Folia Histochem Cytobiol. 2021
10.5603/FHC.a2021.0025
ISSN 0239-8508, e-ISSN 1897-5631

3β protein decreased significantly (Fig. 3C, 4B–D). Taken together, silencing of VDR by high glucose concentration could promote EMT, which could be alleviated by TSIIA treatment through upregulation of VDR expression and inhibition of Wnt/β-catenin signaling pathway. Further, with the reduction of VDR expression in the siVDR and siVDR + HG groups, the further activation of the Wnt/β-catenin pathway was identified. When the expression level of VDR was restored, the Wnt/β-catenin pathway was inhibited again. These results strongly demonstrated that VDR had an inhibitory effect on Wnt/β-catenin pathway, and TSIIA could ameliorate EMT acting on the VDR/Wnt/β-catenin pathway.

Discussion

In this study, we used culture medium with high glucose concentration to induce EMT in HK-2 cells, establishing an *in vitro* EMT model. Our data demonstrated that tanshinone IIA had a significant suppressing effect on EMT in HK-2 cells, and its effect was concentration-dependent. It is well known that hyperglycemia is an essential risk factor for DKD. In the past, DKD has been regarded as a disease mainly characterized by glomerular injury, and the role of renal tubular injury in DKD has been neglected; in recent years, more and more studies have revealed the importance of renal tubulointerstitial injury in the progression of DKD [15]. The main cause of tubulointerstitial fibrosis is renal tubular EMT [16, 17]; therefore, the inhibition of EMT can alleviate tubulointerstitial fibrosis [18]. EMT is a collective name for a series of cellular biological process in which cells differentiate from epithelial cell phenotype into mesenchymal cells phenotype under specific physiological or pathological conditions [19]. The decreased and increased expression of E-cadherin and α-SMA, respectively, are usually considered as markers of EMT. E-cadherin plays an important role in the normal function of epithelial cells [20], while α-SMA can be expressed in myofibroblasts secreting extracellular matrix (ECM) [21]. Studies on tumor cells have shown that the inhibition of E-cadherin protein levels and the increase of α-SMA protein levels promote the migration and invasion of tumor cells [22–24]. Therefore, it has been recognized that increasing the expression and functional activity of E-cadherin [25, 26] and reducing the expression of α-SMA [27] can alleviate tumor progression. This concept has also been applied to attenuate HG- and streptozotocin (STZ)-induced EMT [28, 29]. Consistent with previous studies [30], our results suggested that TSIIA significantly increased the expression of E-cadherin and reduced the expression of α-SMA in HK-2 cells exposed to high glucose concentration, resulting in the alleviation of EMT. This finding may indicate that TSIIA can improve the tubulointerstitial fibrosis by improving the renal tubular epithelial cell EMT, thus improving DKD.

We found that Wnt/β-catenin pathway was involved in EMT induced by culturing the HK-2 kidney proximal tubule cells at high glucose concentration. The pathway was activated in EMT cells induced by high glucose level and siVDR transfection, accompanied by the increase of GSK-3β and β-catenin. The Wnt pathway has been reported to play an important role in renal tubular EMT and renal fibrosis. In the study of Fu *et al.* [31], the Wnt pathway was activated in the progression of EMT and tubulointerstitial lesions. Besides, kallistatin was proved to ameliorate EMT and renal fibrosis by inhibiting the Wnt pathway [32]. In normal condition, the complex in Wnt pathway, degrading β-catenin, is composed of adenomatosis polyposis coli (APC), axin and GSK-3β (Fig. 5). However, in the condition of EMT, extracellular signal molecules activate the Wnt pathway. And β-catenin, as a coactivator of transcription factors, accumulates in the nucleus and activates downstream gene expression, instead of being degraded [33, 34]. Thus, excessive activation of the Wnt pathway may contribute to the progression of renal fibrosis in DKD. Whereas, after treatment with TSIIA, the Wnt pathway was inhibited and EMT was attenuated. The results of our study demonstrate that the inhibition of Wnt pathway is of great significance to improve EMT, and TSIIA may have a therapeutic effect on DKD through this pathway. Other studies illustrated that complete inhibition of the Wnt pathway might also be deleterious to kidney [35]. Therefore, it may be best to keep the pathway in a relatively balanced state, so that it cannot only perform a normal function, but also not be excessive activated. In addition, activation of TGF-β1/Smad [1, 36], NF-kβ [37], PI3K/Akt [38] and other pathways can induce renal tubular EMT and renal fibrosis. Xu *et al.* [39] proved that TSIIA had a protective effect on STZ-induced DKD *via* suppressing PERK pathway-mediated oxidative stress. Wang *et al.* [40] found that TSIIA had anti-fibrotic and anti-inflammatory effects on chronic kidney disease (CKD) rats *via* suppressing TGF-β/Smad and NF-κB pathway. Which pathway plays a decisive role in the protection of TSIIA against renal fibrosis remains to be further studied.

The therapeutic effect of VDR on EMT has been confirmed *in vitro* [41] and animal experiments [42]. However, the relationship between VDR and the Wnt pathway in EMT of DKD has

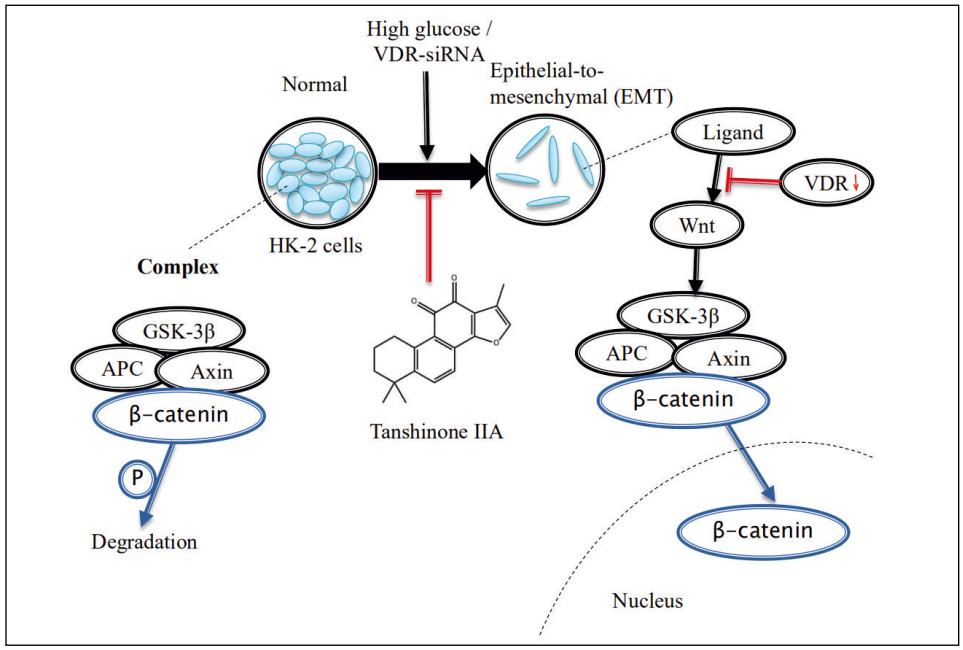

Figure 5. Possible mechanisms of TSIIA action in a cellular EMT model. Under physiological conditions adenomatosis polyposis coli (APC), axin and GSK-3β combine to degrade β-catenin. High glucose and vitamin D receptor (VDR)-siRNA promote EMT and inhibit the degradation of β-catenin in HK-2 cells by downregulating VDR expression. Tanshinone IIA inhibits EMT in HK-2 cells by regulating VDR/Wnt/β-c.

not been clarified. In the present study, the upregulation of VDR could inhibit EMT in an *in vitro* model. Interestingly, we found that VDR may be an upstream regulator of the Wnt pathway. Our results showed that the Wnt pathway changed with the change of VDR. When VDR level is restored, the inhibitory effect of VDR on the Wnt pathway is also restored and the pathway is significantly inhibited. Thus, VDR may be a key protein regulating EMT in DKD.

It is well known that VDR combines with its ligand 1,25 (OH) $_2D_3$ or other analogues to exert biological effects. However, few studies have found that drugs other than VDR ligands and their analogues can affect the level of VDR. It is worth mentioning that the activity of TSIIA in this study can also upregulate VDR, which may mean that TSIIA contains components that can bind and activate VDR. This need to be confirmed by further studies.

There are four limitations in our present study. First, considering that normality test may be inaccurate in the case of small samples, large sample studies on HK-2 cells, and even studies on other cell lines are needed in the future. What's more, the results of *in vitro* experiments cannot be directly applied to clinical trials. Further animal experiments and *in vivo* studies are needed to verify the results. In addition, we used siRNA to reduce VDR expression which only reduced the expression of VDR to a certain extent, so it is not clear whether the Wnt pathway is only regulated by VDR. Finally, since the main purpose of this study is to focus on the therapeutic effect of TSIIA on EMT and the regulatory relationship between VDR and the Wnt pathway, the changes of downstream molecules of this pathway have not been determined, which needs to be found by further experiments.

In conclusion, tanshinone IIA is able to attenuate some high glucose-induced features of EMT in HK2 cells by increasing protein level of VDR, which may be related to the regulation of Wnt pathway by VDR. These results indicate that tanshinone IIA can play a protective role in EMT, which may provide a theoretical basis for further rational use of this drug in the clinical treatment and prevention of DKD.

Author contributions

ZJY and BXR designed the experiments and improved the protocols, ZJY conducted the experiments and wrote the manuscript, BXR revised the manuscript.

Funding

This research did not receive any specific grant from funding agencies in the public, commercial, or not-for-profit sectors.

Data availability statement

The research data that support the findings of this study are included in this article and its supplementary material files. Further enquiries can be directed to the corresponding author.

Conflict of interest

The authors declare that the research was conducted in the absence of any commercial or financial relationships that could be construed as a potential conflict of interest.

References

1. Beshay ON, Ewees MG, Abdel-Bakky MS, et al. Resveratrol reduces gentamicin-induced EMT in the kidney via inhibition of reactive oxygen species and involving TGF-β/Smad pathway. Life Sci. 2020; 258: 118178, doi: 10.1016/j.lfs.2020.118178, indexed in Pubmed: 32739468.
2. Zhou T, Luo M, Cai W, et al. Runt-Related Transcription Factor 1 (RUNX1) Promotes TGF-β-Induced Renal Tubular Epithelial-to-Mesenchymal Transition (EMT) and Renal Fibrosis through the PI3K Subunit p110Δ. EBioMedicine. 2018; 31: 217–225, doi: 10.1016/j.ebiom.2018.04.023, indexed in Pubmed: 29759484.
3. Hu HH, Cao G, Wu XQ, et al. Wnt signaling pathway in aging-related tissue fibrosis and therapies. Ageing Res Rev. 2020; 60: 101063, doi: 10.1016/j.arr.2020.101063, indexed in Pubmed: 32272170.
4. Xie H, Miao N, Xu D, et al. FoxM1 promotes Wnt/β-catenin pathway activation and renal fibrosis via transcriptionally regulating multi-Wnts expressions. J Cell Mol Med. 2021; 25(4): 1958–1971, doi: 10.1111/jcmm.15948, indexed in Pubmed: 33434361.
5. Chen Yu, Chen X, Ji YR, et al. PLK1 regulates hepatic stellate cell activation and liver fibrosis through Wnt/β-catenin signalling pathway. J Cell Mol Med. 2020; 24(13): 7405–7416, doi: 10.1111/jcmm.15356, indexed in Pubmed: 32463161.
6. Kadoya H, Satoh M, Nishi Y, et al. Klotho is a novel therapeutic target in peritoneal fibrosis via Wnt signaling inhibition. Nephrol Dial Transplant. 2020; 35(5): 773–781, doi: 10.1093/ndt/gfz298, indexed in Pubmed: 32221606.
7. Lee DW, Lee WJ, Cho J, et al. Inhibition of Wnt signaling pathway suppresses radiation-induced dermal fibrosis. Sci Rep. 2020; 10(1): 13594, doi: 10.1038/s41598-020-70243-3, indexed in Pubmed: 32788612.
8. Yu M, Wu H, Wang J, et al. Vitamin D receptor inhibits EMT via regulation of the epithelial mitochondrial function in intestinal fibrosis. J Biol Chem. 2021; 296: 100531, doi: 10.1016/j.jbc.2021.100531, indexed in Pubmed: 33713706.
9. Cong, L., Mechanism of vitamin D receptor modulating Wnt/β-catenin signaling pathway in the proliferation and invasion of gastric cancer. 2016, Shandong University.
10. Commission, C.P., Pharmacopoeia of the People's Republic of China. One Edition ed. 2020, Beijing: China: Pharmaceutical Science and Technology Press.
11. Li Y, Gu B, Liu J, et al. Research progress of Tanshinone IIA. Shizhen Guo Yi Guo Yao. 2010; 21(7): 1770–1772, doi: 10.3969/j.issn.1008-0805.2010.07.096.
12. Li Z, Zou J, Cao D, et al. Pharmacological basis of tanshinone and new insights into tanshinone as a multitarget natural product for multifaceted diseases. Biomed Pharmacother. 2020; 130: 110599, doi: 10.1016/j.biopha.2020.110599, indexed in Pubmed: 33236719.
13. Feng J, Chen HW, Pi LJ, et al. Protective effect of tanshinone IIA against cardiac hypertrophy in spontaneously hypertensive rats through inhibiting the Cys-C/Wnt signaling pathway. Oncotarget. 2017; 8(6): 10161–10170, doi: 10.18632/oncotarget.14328, indexed in Pubmed: 28053285.
14. Li ZY, Huang GD, Chen L, et al. Tanshinone IIA induces apoptosis via inhibition of Wnt/βcatenin/MGMT signaling in AtT20 cells. Mol Med Rep. 2017; 16(5): 5908–5914, doi: 10.3892/mmr.2017.7325, indexed in Pubmed: 28849207.
15. Chen SJ, Lv LL, Liu BC, et al. Crosstalk between tubular epithelial cells and glomerular endothelial cells in diabetic kidney disease. Cell Prolif. 2020; 53(3): e12763, doi: 10.1111/cpr.12763, indexed in Pubmed: 31925859.
16. Li X, Zhang F, Qu L, et al. Identification of YAP1 as a novel downstream effector of the FGF2/STAT3 pathway in the pathogenesis of renal tubulointerstitial fibrosis. J Cell Physiol. 2021; 236(11): 7655–7671, doi: 10.1002/jcp.30415, indexed in Pubmed: 33993470.
17. Chan SC, Zhang Y, Shao A, et al. Mechanism of Fibrosis in -Related Autosomal Dominant Tubulointerstitial Kidney Disease. J Am Soc Nephrol. 2018; 29(10): 2493–2509, doi: 10.1681/ASN.2018040437, indexed in Pubmed: 30097458.
18. Zhang Bo, Ru F, Chen X, et al. Autophagy attenuates renal fibrosis in obstructive nephropathy through inhibiting epithelialtomesenchymal transition. Zhong Nan Da Xue Xue Bao Yi Xue Ban. 2021; 46(6): 601–608, doi: 10.11817/j.issn.1672-7347.2021.201008, indexed in Pubmed: 34275928.
19. Jonckheere S, Adams J, De Groote D, et al. Epithelial-Mesenchymal Transition (EMT) as a Therapeutic Target. Cells Tissues Organs. 2021 [Epub ahead of print]: 1–26, doi: 10.1159/000512218, indexed in Pubmed: 33401271.
20. Bruner HC, Derksen PWB. Loss of E-Cadherin-Dependent Cell-Cell Adhesion and the Development and Progression of Cancer. Cold Spring Harb Perspect Biol. 2018; 10(3), doi: 10.1101/cshperspect.a029330, indexed in Pubmed: 28507022.
21. Ding H, Chen J, Qin J, et al. TGF-β-induced α-SMA expression is mediated by C/EBPβ acetylation in human alveolar epithelial cells. Mol Med. 2021; 27(1): 22, doi: 10.1186/s10020-021-00283-6, indexed in Pubmed: 33663392.
22. Wang YP, Wang QY, Li CH, et al. COX-2 inhibition by celecoxib in epithelial ovarian cancer attenuates E-cadherin suppression through reduced Snail nuclear translocation. Chem Biol Interact. 2018; 292: 24–29, doi: 10.1016/j.cbi.2018.06.020, indexed in Pubmed: 29932878.
23. Liu B, Li X, Li C, et al. miR-25 mediates metastasis and epithelial-mesenchymal-transition in human esophageal squamous cell carcinoma via regulation of E-cadherin signaling. Bioengineered. 2019; 10(1): 679–688, doi: 10.1080/21655979.2019.1687391, indexed in Pubmed: 31679450.
24. Zhan S, Liu Z, Zhang M, et al. Overexpression of B7-H3 in α-SMA-Positive Fibroblasts Is Associated With Cancer Progression and Survival in Gastric Adenocarcinomas. Front Oncol. 2019; 9: 1466, doi: 10.3389/fonc.2019.01466, indexed in Pubmed: 31998637.
25. Na TY, Schecterson L, Mendonsa AM, et al. The functional activity of E-cadherin controls tumor cell metastasis at multiple steps. Proc Natl Acad Sci U S A. 2020; 117(11): 5931–5937, doi: 10.1073/pnas.1918167117, indexed in Pubmed: 32127478.
26. Li XR, Jin JJ, Yu Y, et al. PET-CT radiomics by integrating primary tumor and peritumoral areas predicts E-cadherin

expression and correlates with pelvic lymph node metastasis in early-stage cervical cancer. Eur Radiol. 2021; 31(8): 5967–5979, doi: 10.1007/s00330-021-07690-7, indexed in Pubmed: 33528626.
27. Masuda T, Nakashima T, Namba M, et al. Inhibition of PAI-1 limits chemotherapy resistance in lung cancer through suppressing myofibroblast characteristics of cancer-associated fibroblasts. J Cell Mol Med. 2019; 23(4): 2984–2994, doi: 10.1111/jcmm.14205, indexed in Pubmed: 30734495.
28. Wang YN, Zhao SL, Su YY, et al. Astragaloside IV attenuates high glucose-induced EMT by inhibiting the TGF-β/Smad pathway in renal proximal tubular epithelial cells. Biosci Rep. 2020; 40(6), doi: 10.1042/BSR20190987, indexed in Pubmed: 32515466.
29. Wang WW, Liu YL, Wang MZ, et al. Inhibition of Renal Tubular Epithelial Mesenchymal Transition and Endoplasmic Reticulum Stress-Induced Apoptosis with Shenkang Injection Attenuates Diabetic Tubulopathy. Front Pharmacol. 2021; 12: 662706, doi: 10.3389/fphar.2021.662706, indexed in Pubmed: 34408650.
30. Cao L, Huang B, Fu X, et al. Effects of tanshinone IIA on the regulation of renal proximal tubular fibrosis. Mol Med Rep. 2017; 15(6): 4247–4252, doi: 10.3892/mmr.2017.6498, indexed in Pubmed: 28440499.
31. Fu D, Senouthai S, Wang J, et al. FKN Facilitates HK-2 Cell EMT and Tubulointerstitial Lesions via the Wnt/β-Catenin Pathway in a Murine Model of Lupus Nephritis. Front Immunol. 2019; 10: 784, doi: 10.3389/fimmu.2019.00784, indexed in Pubmed: 31134047.
32. Yiu WH, Li Ye, Lok SWY, et al. Protective role of kallistatin in renal fibrosis via modulation of Wnt/β-catenin signaling. Clin Sci (Lond). 2021; 135(3): 429–446, doi: 10.1042/CS20201161, indexed in Pubmed: 33458750.
33. Xiong Y, Zhou L. The Signaling of Cellular Senescence in Diabetic Nephropathy. Oxid Med Cell Longev. 2019; 2019: 7495629, doi: 10.1155/2019/7495629, indexed in Pubmed: 31687085.
34. Shi M, Tian P, Liu Z, et al. MicroRNA-27a targets Sfrp1 to induce renal fibrosis in diabetic nephropathy by activating Wnt/β-Catenin signalling. Biosci Rep. 2020; 40(6), doi: 10.1042/BSR20192794, indexed in Pubmed: 32484208.
35. Guo Q, Zhong W, Duan A, et al. Protective or deleterious role of Wnt/beta-catenin signaling in diabetic nephropathy: An unresolved issue. Pharmacol Res. 2019; 144: 151–157, doi: 10.1016/j.phrs.2019.03.022, indexed in Pubmed: 30935943.
36. Ai K, Zhu X, Kang Ye, et al. miR-130a-3p inhibition protects against renal fibrosis in vitro via the TGF-β1/Smad pathway by targeting SnoN. Exp Mol Pathol. 2020; 112: 104358, doi: 10.1016/j.yexmp.2019.104358, indexed in Pubmed: 31836508.
37. Perretta-Tejedor N, Muñoz-Félix JM, Düwel A, et al. Cardiotrophin-1 opposes renal fibrosis in mice: Potential prevention of chronic kidney disease. Acta Physiol (Oxf). 2019; 226(2): e13247, doi: 10.1111/apha.13247, indexed in Pubmed: 30589223.
38. Higgins DF, Ewart LM, Masterson E, et al. BMP7-induced-Pten inhibits Akt and prevents renal fibrosis. Biochim Biophys Acta Mol Basis Dis. 2017; 1863(12): 3095–3104, doi: 10.1016/j.bbadis.2017.09.011, indexed in Pubmed: 28923783.
39. Xu S, He L, Ding K, et al. Tanshinone IIA Ameliorates Streptozotocin-Induced Diabetic Nephropathy, Partly by Attenuating PERK Pathway-Induced Fibrosis. Drug Des Devel Ther. 2020; 14: 5773–5782, doi: 10.2147/DDDT.S257734, indexed in Pubmed: 33408464.
40. Wang DT, Huang RH, Cheng X, et al. Tanshinone IIA attenuates renal fibrosis and inflammation via altering expression of TGF-β/Smad and NF-κB signaling pathway in 5/6 nephrectomized rats. Int Immunopharmacol. 2015; 26(1): 4–12, doi: 10.1016/j.intimp.2015.02.027, indexed in Pubmed: 25744602.
41. Zhang F.X. The role of VDR on epithelial-mesenchymal transition induced by high glucose of Mice Podocyte. 2016, Zhengzhou University.
42. Guo J, Lu C, Zhang F, et al. VDR Activation Reduces Proteinuria and High-Glucose-Induced Injury of Kidneys and Podocytes by Regulating Wnt Signaling Pathway. Cell Physiol Biochem. 2017; 43(1): 39–51, doi: 10.1159/000480315, indexed in Pubmed: 28848172.

Submitted: 9 September, 2021
Accepted after reviews: 6 November, 2021
Available as AoP: 30 December, 2021